Observation of Anomalous Spin Segregation in a Trapped Fermi Gas

X. Du, L. Luo, B. Clancy, and J. E. Thomas*
Department of Physics, Duke University, Durham, North Carolina 27708, USA
(Received 7 May 2008; published 6 October 2008)

We report the observation of spin segregation, i.e., time-dependent separation of the spin density profiles of two spin states, in a trapped, coherently prepared Fermi gas of ^{6}Li with a magnetically tunable scattering length a_{12} close to zero. For $|a_{12}| \simeq 5$ bohr, as the cloud profiles evolve, the measured difference in the densities at the cloud center increases in 200 ms from 0 to $\simeq 60\%$ of the initial mean density and changes sign with a_{12}. The data are in disagreement in both amplitude and temporal evolution with a spin-wave theory for a Fermi gas. In contrast, for a Bose gas, an analogous theory has successfully described previous observations of spin segregation. The observed segregated atomic density profiles are far from equilibrium, yet they persist for $\simeq 5$ s, long compared to the axial trapping period of 6.9 ms. We find the zero crossing in $a_{12} = 0$, where spin segregation ceases, at 527.5 ± 0.2 G.

DOI: 10.1103/PhysRevLett.101.150401 PACS numbers: 03.75.Ss

Ultracold Fermi gases near a collisional (Feshbach) resonance [1] exhibit strong interactions [2] and offer unprecedented opportunities to test nonperturbative quantum many-body theory in systems from high temperature superconductors to nuclear matter. Near the resonance, a bias magnetic field tunes the interaction between two spin states from strongly repulsive to strongly attractive. These strongly interacting Fermi gases have been extensively studied over the past few years [3]. In contrast, the weakly interacting regime of a Fermi gas near a zero crossing of a Feshbach resonance has received relatively little attention. In this regime, the *s*-wave scattering length for atoms in opposite spin states can be tuned smoothly from small and positive to small and negative as a bias magnetic field is varied.

We report the observation of anomalous spin segregation in an optically trapped Fermi gas of ^{6}Li with a bias magnetic field near 528 G, close to the zero crossing of the scattering length a_{12}. The sample is prepared in a coherent superposition of the two lowest energy spin states $|1\rangle$ and $|2\rangle$, with equal populations and the same atomic density profiles. After several hundred milliseconds, the spatial densities segregate strongly, with one spin state moving outward and one moving inward, as shown in Fig. 1. Segregation does not occur in incoherent mixtures. Previously, a theory of overdamped longitudinal spin waves [4–6] has been used to explain the spin segregation that was observed in a Bose gas [7]. The corresponding theory for a Fermi gas correctly predicts our observation that the roles of the spin states are interchanged when the sign of a_{12} is reversed. However, for the conditions of our experiments, this theory predicts a maximum $\simeq 0.2\%$ difference in the densities of the two spin states at the cloud center that oscillates at a rate near the axial trap frequency of 145 Hz. In contrast, we observe a maximum difference of $\simeq 60\%$ that builds up slowly over 200 ms and decays over several seconds.

In the experiments, a sample of ^{6}Li atoms in a 50/50 mixture of the two lowest hyperfine states is loaded into a CO_2 laser trap with a bias magnetic field of 840 G, where the two states are strongly interacting. Evaporative cooling is performed to lower the temperature of the sample [2]. The magnetic field is then increased in 0.8 s to a weakly interacting regime at 1200 G, where an on-resonance optical pulse of 15 μs is applied to remove atoms of one state while leaving atoms in the other state intact. With the single state present, the magnetic field is lowered in 0.8 s to 528 G, near the zero crossing. Then an rf pulse is applied on the $|1\rangle - |2\rangle$ transition to create spin coherence. We determine the Rabi frequency to be $\simeq$120 Hz by observing coherent oscillations in the population for a resonant rf pulse. However, to obtain long term stability in the experiments, we sweep the frequency by 35 kHz during a 40 ms rf pulse in order to transfer about 50% of the atoms. The rf frequency sweep is centered at the hyperfine transition frequency ~75 MHz at 528 G. Note that, as the frequency passes through resonance, coherence is created on a time scale of a few milliseconds, short compared to the time for the total sweep and for spin segregation to occur. We control the amplitude of the spin transfer by varying the sweep rate. Finally, we take absorption images of atoms in both states (in separate experimental cycles) at various times after the swept rf pulse. Each cloud profile is obtained 400 μs after release of the cloud, permitting the cloud to expand in the radial direction for improved imaging, while the axial distribution changes negligibly.

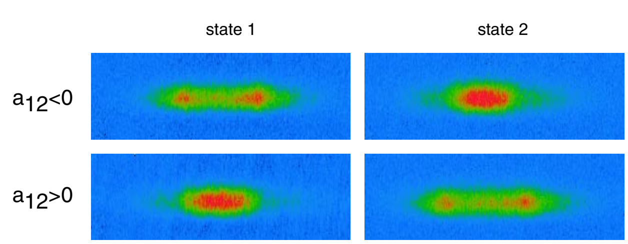

FIG. 1 (color online). Absorption images (states 1 and 2) taken at 200 ms after the rf pulse for 526.2 (scattering length $a_{12} < 0$) and 528.8 G ($a_{12} > 0$). Each image is 1.2 mm in the horizontal direction.

At the final optical trap depth, the measured trap oscillation frequency in the transverse directions is $\omega_\perp = 2\pi \times 4360$ Hz, while the axial frequency is $\omega_z = 2\pi \times 145$ Hz at 528 G. The total number of atoms is $N \simeq 2.0 \times 10^5$. The corresponding Fermi temperature is $T_F \simeq 7$ μK. The trapping potentials U_1 and U_2 for atoms in the two states differ slightly in the axial direction, due to the small difference in their magnetic moments and the magnetic field curvature, which we determine by measuring the magnetic field-dependent axial trapping frequency for shallow optical traps. We find $d^2[(U_1 - U_2)/h]/dz^2 = 4.4 \times 10^{-4}$ Hz$/\mu$m^2. As in the Bose gas studies [7], the difference in the trapping potentials of the two states is 4 orders of magnitude smaller than the thermal energy $k_B T$ and cannot account for our observations.

We find that the spin segregation is not sensitive to the temperature of the cloud. We observe spin segregation over the range from a degenerate Fermi gas ($T \simeq 0.15 T_F$) to a nondegenerate one ($T \simeq 4T_F$). All of the data shown in this Letter were taken in the nondegenerate regime.

The experimental results for spin segregation as a function of bias magnetic field are summarized in Fig. 2(a). Note that the magnetic fields are precisely calibrated with an rf spectroscopic technique, as described below. In Fig. 2, the sample temperature is $T \simeq 27$ μK, and the peak atomic density is $1.2 \times 10^{12}/\text{cm}^3$. The axial $1/e$ width for a fit of a Gaussian distribution to the initial density profile of the trapped cloud is $\simeq$300 μm. For this axial size, the hyperfine transition frequency varies by $\simeq$20 Hz across the sample. From the measured trap frequencies and the axial width, the estimated radial $1/e$ width of the trapped cloud is 10 μm. The corresponding variation in the transition frequency is negligible.

Spin segregation observed in an ultracold Bose gas [7] has been described previously as an overdamped spin wave [4–6]. The basic idea can be described in terms of a Bloch vector. We take the axis w as the "longitudinal" population inversion and the axes u and v as the "transverse" coherence. An rf pulse prepares a coherent superposition of spin up and spin down with polarization in the u-v plane. As noted above, the hyperfine transition frequency varies along the long axial direction of the sample by $\sim$20 Hz. After the rf pulse, the inhomogeneous precession of the Bloch vectors about the w axis starts to build up a spin orientation gradient in u-v plane along the axial direction. Meanwhile, atoms with different spins move around and collide with each other. The interaction due to the binary collision leads to precession of each atom's spin about the total spin vector of both atoms. Since both atoms have spins in u-v plane, the precession of each spin about the total spin in u-v plane produces spin components *out* of the u-v plane. The subsequent formation of a w component leads to a spatially varying population inversion and accounts for the spin segregation.

We tried to use a spin-wave theory to explain the spin segregation observed in our experiment. We derived equations for the spin density and spin current using a Wigner function operator approach [8]. The Wigner phase space operators are written in terms of position space creation and annihilation operators

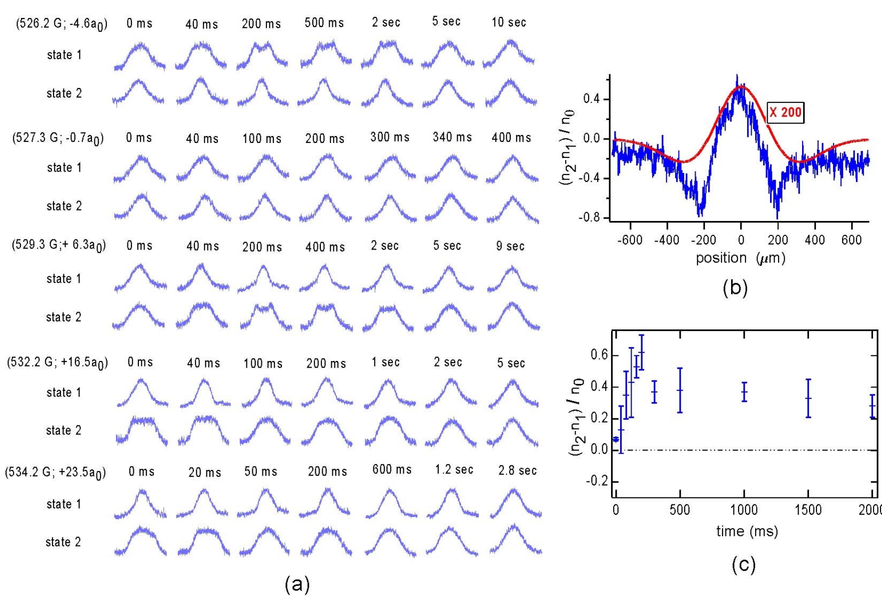

FIG. 2 (color online). (a) Axial atomic density profiles n_1 and n_2 (integrated over transverse directions) versus time relative to the end of the rf pulse for different magnetic fields and scattering lengths (B, a_{12}). a_{12} is estimated with $a_{12}(B) = \acute{a}(B - B_0)$, where $\acute{a} = 3.5 a_0/\text{G}$ [13,14] and $B_0 = 527.5$ G is the zero crossing measured in the experiments. Note that different graphs have different time scales; (b) $n_2 - n_1$ at 200 ms for $B = 526.2$ G in units of $n_0 = (n_{10} + n_{20})/2$. Here n_{i0} is the spin density for state $i = 1, 2$ at the trap center before spin segregation occurs. The solid red curve is the prediction at maximum segregation multiplied by a factor of 200, which oscillates in time with a period of $\simeq 7$ ms, inconsistent with our observations; (c) $n_2 - n_1$ at the trap center versus time for $B = 526.2$ G. The spin density relaxes back to equilibrium at 10 s.

$$\hat{W}_{\alpha\alpha'}(\mathbf{r},\mathbf{p}) \equiv \int \frac{d^3\boldsymbol{\epsilon}}{(2\pi\hbar)^3} e^{i\mathbf{p}\cdot\boldsymbol{\epsilon}/\hbar} \hat{\psi}^+_{\alpha'}\left(\mathbf{r}+\frac{\boldsymbol{\epsilon}}{2}\right)\hat{\psi}_\alpha\left(\mathbf{r}-\frac{\boldsymbol{\epsilon}}{2}\right). \quad (1)$$

The Heisenberg equations are $\dot{\hat{W}}_{\alpha\alpha'}(\mathbf{r},\mathbf{p}) = \frac{i}{\hbar} \times [\hat{H}, \hat{W}_{\alpha\alpha'}(\mathbf{r},\mathbf{p})]$, where $\hat{H}$ is the Hamiltonian operator

$$\hat{H} = \sum_j \int d^3\mathbf{r}\hat{\psi}^+_j(\mathbf{r})\left[-\frac{\hbar^2}{2m}\nabla^2 + U_j + \hbar\omega_j\right]\hat{\psi}_j(\mathbf{r}) + \sum_{j,k}\int d^3\mathbf{r}_1 \int d^3\mathbf{r}_2 \hat{\psi}^+_j(\mathbf{r}_1)\hat{\psi}^+_k(\mathbf{r}_2)u_{jk}(\mathbf{r}_1-\mathbf{r}_2) \times \hat{\psi}_k(\mathbf{r}_2)\hat{\psi}_j(\mathbf{r}_1),$$

with $U_j = \frac{1}{2}m\omega_\perp^2(x^2+y^2) + \frac{1}{2}m\omega_{zj}^2 z^2$ and $u_{jk}(\mathbf{r}_1 - \mathbf{r}_2) = \frac{1}{2}\hbar g_{jk}\delta(\mathbf{r}_1-\mathbf{r}_2)$. Here j and k refer to states $|1\rangle$ or $|2\rangle$; U_j is the total external potential (combined optical and magnetic) for atoms in state j; $\hbar\omega_j$ is hyperfine energy of state j; $g_{jk} = 4\pi\hbar a_{jk}/m$, with m the atomic mass; a_{jk} is the scattering length for atoms between state j and state k.

Spin density operators $\hat{s}_x = [\hat{\psi}^+_1(\mathbf{r})\hat{\psi}_2(\mathbf{r}) + \text{H.c.}]/2$, etc., can be written in terms of the momentum integral of the Wigner phase space operators: $\int \hat{W}_{\alpha\alpha'}(\mathbf{r},\mathbf{p})d^3\mathbf{p} = \hat{\psi}^+_{\alpha'}(\mathbf{r})\hat{\psi}_\alpha(\mathbf{r})$. The corresponding spin current operators are obtained from $\int(\mathbf{p}/m)\hat{W}_{\alpha\alpha'}(\mathbf{r},\mathbf{p})d^3\mathbf{p}$.

We obtain the spin-wave equations for both a Bose gas and a Fermi gas:

$$\frac{\partial S^{(i)}}{\partial t} + \nabla\cdot\mathbf{J}^{(i)} = (\boldsymbol{\Omega}\times\mathbf{S})^{(i)},$$
$$\frac{\partial \mathbf{J}^{(i)}}{\partial t} + \alpha\nabla S^{(i)} = (\boldsymbol{\Omega}'\times\overleftrightarrow{J})^{(i)} - \gamma\mathbf{J}^{(i)} - \frac{1}{2m}S^{(i)}\nabla U - \frac{1}{4m}n\nabla U'^{(i)}, \quad (2)$$

where $\boldsymbol{\Omega} = (\omega_0 + \delta\omega_1 + \delta\omega_2)\hat{z}$, $\delta\omega_1 = (U_1 - U_2)/\hbar$, $\delta\omega_2 = 2g_{11}n_1 - 2g_{22}n_2 - 2(\epsilon+1)g_{12}S^{(z)}$, $\boldsymbol{\Omega}' = \boldsymbol{\Omega} + 2\epsilon g_{12}\mathbf{S}$, $U = U_1 + U_2 + 2\hbar g_{11}n_1 + 2\hbar g_{22}n_2 + \hbar g_{12}n$, and $\mathbf{U}' = \hbar\boldsymbol{\Omega}'$. $S^{(i)}$ is the spin density component in direction $i = x, y, z$. For example, $S^{(z)} = (n_1 - n_2)/2$, with n_1 and n_2 the atom densities in states $|1\rangle$ and $|2\rangle$, respectively. $\mathbf{J}^{(i)}$ is the spin current corresponding to spin component i [9]. $\omega_0/2\pi$ is the hyperfine transition frequency. n is the total atom density, $\alpha = k_BT/m$, and γ is the relaxation rate. $\epsilon = +1(-1)$ for bosons (fermions), and $a_{11} = a_{22} = 0$ for fermions.

Numerical simulations based on these equations quantitatively reproduce prior calculations of spin segregation in Bose gases [4–6] that agree with the experiments [7]. In the Bose gas experiments, the times for spin segregation and for the cloud to relax were comparable to the axial trap period of 160 ms, and $g_{12}n = 2\pi \times 140$ Hz. For the conditions of our experiments in Fermi gases (axial trap frequency 145 Hz, $g_{12}n = 2\pi \times 7$ Hz at $B = 526.2$ G), the spin-wave equations correctly predict the inversion of the roles of the spins when the scattering length a_{12} is reversed in sign. However, the theory predicts that the difference in the spin density profiles oscillates with a period of 6.9 ms, close to the axial period. In contrast, for measurements on a millisecond time scale, we observe no oscillation. Further, as shown in Fig. 2(b), the simulation (solid red curve) is a factor of 200 smaller than the data. Here we assumed that the coherence was created instantaneously at time $t = 0$, and we show the result at $t = 3.2$ ms where the maximum occurs. The observed difference in the densities smoothly increases over 200 ms before relaxing back to equilibrium over several seconds as shown in Fig. 2(c), in contrast to the oscillatory prediction. Since the relaxation time is several seconds in our experiments, the simulation is insensitive to the choice of γ, and we show the curve for $\gamma = 0$ in Fig. 2(b).

Figure 2(a) also shows that the time for the cloud to relax back to its original density profile increases as the scattering length is reduced in magnitude. For example, at 526.2 G, where the scattering length is about $-4.6a_0$, spin segregation can be maintained for up to 5 s, although the trap axial period is 6.9 ms. This result is strikingly longer than that observed in the previous experiments with a Bose gas [7], where the spin densities relaxed from maximum segregation back to their original profiles on a time scale of the axial trap period, $\simeq 200$ ms. We attribute the long time scales to the facts that ultracold fermionic ^{6}Li atoms interact only via s-wave scattering between *opposite* spin states and that the ^{6}Li scattering length a_{12} near the zero crossing is $-4.6a_0$, much smaller than for the Bose gas experiments, where $a_{12} \sim 100a_0$ for ^{87}Rb.

Spin segregation is difficult to observe when the magnetic field is too close to the zero crossing, for example, 527.3 G in Fig. 2(a), where $a_{12} = -0.7a_0$, as the segregation time is very long and far exceeds the decoherence time. We have measured the decoherence time by observing the net population transfer as a function of time delay between two time-separated rf pulses and obtained 70 ms, comparable to the longest spin segregation time of 200 ms that we observe. This decoherence time is consistent with the estimated frequency inhomogeneity of 20 Hz across the sample. Spin segregation is also difficult to observe very far from the zero crossing, $\sim$15 G above or below. Here the scattering length is large, and collisional relaxation is fast compared to the time for spin segregation.

In an additional experiment, we create a sample that reaches the maximum spin segregation in 200 ms at 529 G. Then we immediately blow out atoms of one state using a resonance optical pulse and take images of the remaining state at various times after the optical pulse. The profile of the remaining state decays in $\sim$2 s, demonstrating that slow relaxation of one state does not depend on the presence of the other state. The double-peak and one-peak non-Gaussian atomic density profiles observed in our experiments are far from equilibrium. It is remarkable that we can create a nonequilibrium stationary system that has such

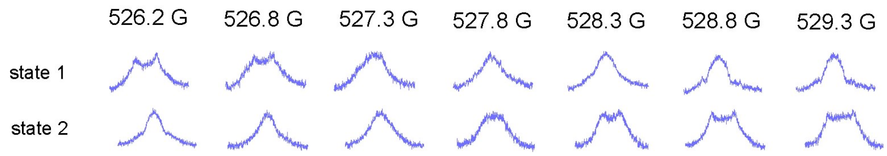

FIG. 3 (color online). Axial atomic density profiles at 200 ms after coherence is created by an rf pulse, for different magnetic fields. The zero crossing point in the scattering length is determined by observing the change in the sign of the difference in the spin densities as the magnetic field is varied.

a long lifetime ($\sim$2 s) compared to the axial trap period 6.9 ms and segregation time $\sim$200 ms.

Previous experiments have shown that a zero crossing occurs in the $|1\rangle - |2\rangle$ scattering length of ^{6}Li near 528 G [10,11]. We now describe a new determination of the zero crossing based on the behavior of the spin segregation as the magnetic field is varied. As described above, the roles of the spin states are interchanged as the scattering length a_{12} changes sign from negative to positive. Figure 2(a) shows data for $a_{12} < 0$ at 526.2 G and for $a_{12} > 0$ at 529.3 G. Taking advantage of the fact that spin segregation slows for magnetic fields very close to the zero crossing, we determine the zero crossing precisely. We take absorption images of both states at 200 ms after the rf pulse for different magnetic fields. Figure 3 shows a clear change in the spin segregation behavior from 526.2 to 529.3 G. The magnetic fields are calibrated by rf spectroscopy using the Hamiltonian for the ^{6}Li ground state hyperfine interactions in a magnetic field:

$$H_{\rm int} = \frac{a_{\rm hf}}{\hbar^2}\mathbf{S}\cdot\mathbf{I} - \frac{\mu_B}{\hbar}(g_J\mathbf{S} + g_I\mathbf{I})\cdot\mathbf{B}, \qquad (3)$$

where $\mu_B/h = 1.399\,624\,604$ MHz is the Bohr magneton, $a_{\rm hf}/h = 152.136\,840\,7$ MHz [12] is the ground state magnetic hyperfine constant for ^{6}Li, $g_J = -2.002\,301\,0$ [12] is the total electronic g factor for the ^{6}Li ground state, $g_I = 0.000\,447\,654\,0$ [12] is the nuclear g factor, h is Planck's constant, and $\mathbf{B}$ is the bias magnetic field.

The transition in the behavior of the segregation occurs at 527.5 G, which is determined as follows. We fit the axial atomic density profiles of both states with a Gaussian distribution for the data taken at 527.3 and 527.8 G. For each data set, we derive Gaussian widths of both clouds and their ratio. The ratio of the width of state $|1\rangle$ to that of state $|2\rangle$ is greater than 1 for 527.3 G and less than 1 for 527.8 G. By interpolation, we find the point where the ratio of widths is equal to 1, which determines the value of magnetic field 527.5 $\pm$ 0.2 G (the error bar is the quadratic combination of the shot-to-shot fluctuation of the magnetic field setting and the magnetic field calibration error arising from the rf spectrum fit). Since no spin segregation occurs with the scattering length of zero, we interpret the value of magnetic field where the ratio of widths is 1 to be the zero crossing.

In conclusion, we have observed spin segregation in a trapped ultracold atomic Fermi gas of ^{6}Li with a scattering length close to zero. The large discrepancies between the observed and predicted spin segregation for the conditions of our experiments appear to require a modification of the current theory based on spin waves or possibly a new mechanism. A possible explanation may involve the very small scattering length a_{12} and correspondingly long relaxation time to thermal equilibrium, which may lead to a violation of the factorization assumption (Wick's theorem) used to derive the spin-wave equations. In addition, using spin segregation, we have precisely determined the zero crossing in the scattering length of ^{6}Li.

This research is supported by the Physics Divisions of the Army Research Office and the National Science Foundation, and the Chemical Sciences, Geosciences and Biosciences Division of the Office of Basic Energy Sciences, Office of Science, U.S. Department of Energy. We thank Yueheng Lan (UCSB) for help in numerical modeling.

*jet@phy.duke.edu

[1] E. Tiesinga, A. J. Moerdijk, B. J. Verhaar, and H. Stoof, Phys. Rev. A **46**, R1167 (1992); E. Tiesinga, B. J. Verhaar, and H. Stoof, Phys. Rev. A **47**, 4114 (1993).
[2] K. M. O'Hara *et al.*, Science **298**, 2179 (2002).
[3] S. Giorgini, L. P. Pitaevskii, and S. Stringari, arXiv:0706.3360 [Rev. Mod. Phys. (to be published)].
[4] M. Ö. Oktel and L. S. Levitov, Phys. Rev. Lett. **88**, 230403 (2002).
[5] J. N. Fuchs, D. M. Gangardt, and F. Laloë, Phys. Rev. Lett. **88**, 230404 (2002).
[6] J. E. Williams, T. Nikuni, and Charles W. Clark, Phys. Rev. Lett. **88**, 230405 (2002).
[7] H. J. Lewandowski *et al.*, Phys. Rev. Lett. **88**, 070403 (2002).
[8] J. E. Thomas and L. J. Wang, Phys. Rep. **262**, 311 (1995).
[9] $\underset{\sim}{J}$ is a tensor, and $\mathbf{J}^{\mathbf{i}}$ is a vector in coordinate space.
[10] K. M. O'Hara *et al.*, Phys. Rev. A **66**, 041401(R) (2002).
[11] S. Jochim *et al.*, Phys. Rev. Lett. **89**, 273202 (2002).
[12] E. Arimondo, M. Inguscio, and P. Violino, Rev. Mod. Phys. **49**, 31 (1977).
[13] M. Bartenstein *et al.*, Phys. Rev. Lett. **94**, 103201 (2005).
[14] P. S. Julienne (private communication).